JOURNAL OF CATALYSIS 55, 361–372 (1978)

Oxidation of Butene to Maleic Anhydride

I. Kinetics and Mechanism

R. L. VARMA[1] AND D. N. SARAF[2]

Department of Chemical Engineering, Indian Institute of Technology, Kanpur-208016, India

Received December 13, 1977; revised July 27, 1978

Selective oxidation of butene to maleic anhydride over a vanadyl phosphate catalyst has been investigated in a quasi-isothermal integral reactor at temperatures between 350 and 390°C. Maleic anhydride, butadiene, and carbon oxides are the main oxidation products. Kinetic data obtained supported a two-stage redox model. Data obtained under conditions of low partial pressures of butene could be analyzed in terms of pesudo-first-order kinetics. The analysis of the reaction network revealed no significant destruction of maleic anhydride to carbon oxides under the reaction conditions studied. The derived rate expressions gave satisfactory fit to the experimental data.

INTRODUCTION

The selective oxidation of C_4 hydrocarbons to maleic anhydride is economically quite attractive mainly owing to the low cost of feed stock (*1, 2*). In view of the advantages of the C_4 process over the conventional benzene oxidation, considerable effort has been devoted to oxidation of the butene–butane fraction. This is evident from the numerous patents issued on the process in recent years (*3*). Although various catalysts for the reaction have been suggested, meager information is available in the literature on kinetics (*4*).

Dente *et al.* (*5*) examined the kinetics of oxidation of butene and butadiene to maleic anhydride and formaldehyde on a Fe–Mo-oxide catalyst although more selective catalysts are known for this reaction. For example, catalysts containing oxides of vanadium and phosphorus have been described by a majority of investigators in the patent literature to be remarkably selective to maleic anhydride formation (*3, 4*). The structure and activity of V–PO catalysts have been studied by Nakamura *et al.* (*6*). The effect of phosphorus addition to the vanadium catalyst during oxidation of butene has been studied by Ai and co-workers (*7, 8*).

The mechanism of formation of maleic anhydride from butene has been proposed by Sampson and Shooter (*9*), Ostroushko *et al.* (*10*), and Ai *et al.* (*11*). It is suggested (*10, 11*) that over V–P-oxide catalyst, maleic anhydride is obtained from *n*-butenes via 1,3-butadiene and furan. Crotonaldehyde has also been postulated to be an intermediate product during step-by-step oxidation (*12, 13*), although this possibility has been ruled out by recent investigators (*10*). Butadiene has been found to be a primary intermediate product (*7*).

Recently Sunderland (*14*) studied the kinetics of 2-butene oxidation to maleic

---

[1] Present address: Harcourt Butler Technological Institute, Kanpur, India.

[2] To whom correspondence should be sent.

0021-9517/78/0553-0361$02.00/0

anhydride in a recycle reactor in the temperature range 573 to 623 K. Rate expressions were proposed for each step in the overall reaction scheme represented as

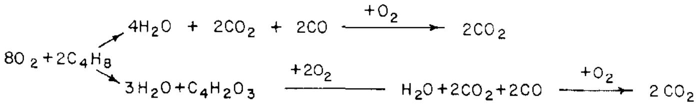

It should be noted, however, that the usual temperature for this reaction has been reported to be above 623 K in almost all the patent claims and published works pertaining to this process (*3*, *4*, *15*, *16*).

This work deals with the kinetic study of this multiple reaction over a V–P–O catalyst in the temperature range 623 to 663 K. It is shown that significantly different behavior may be expected at higher temperatures.

NOTATION

A_i	The *i*th component in a chemical reaction network (listed in Table 1)
A_j^0	Preexponential factor in the Arrhenius rate expression for reaction step *j*
E_j	Activation energy for reaction step *j* (kcal/g-mole)
F_t	Total molar flow rate (g-moles/sec)
F_{o1}	Molar flow rate of component A_1 in feed (g-moles/sec)
k_h	Reaction rate constant for hydrocarbon (g-moles/g-cat atm sec)
k_o	Rate constant for oxygen adsorption (g-moles/g-cat atm sec)
k_j	Reaction rate constant for reaction step *j* (g-moles/g-cat atm sec)
M	Number of data points
N_{o1}	Mole fraction of component A_1 in feed (F_{o1}/F_t)
N	Number of species
P	Total pressure (atm)
p_h	Partial pressure of hydrocarbon (atm)
p_o	Partial pressure of oxygen (atm)
p_i	Partial pressure of component A_i (atm)
p_{o1}	Partial pressure of component A_1 in feed (atm)
R_h	Rate of hydrocarbon oxidation (g-moles/g-cat sec)
W	Weight of catalyst (g)
Y_{ij}	Measured yield of component *i* at time τ_j
$\hat{Y}_{ij}$	Yield of component *i* at time τ_j, computed by Eqs. (15) to (17)
α_o	Average number of moles of oxygen required per mole of hydrocarbon oxidation (stoichiometric number)
τ_1	Time factor based on hydrocarbon feed rate, W/F_1 (g-cat sec/g-mole)

EXPERIMENTAL METHODS

Catalyst

The V–PO catalyst (P:V atomic ratio, 1.6) used was made as follows. Ammonium metavanadate (NH_4VO_3; 57.5 g) mixed with reducing agents (120 g of oxalic acid + 100 ml of hydrochloric acid) was dissolved in water and the mixture refluxed, until 600 ml of clear blue solution was obtained. To this solution 55.9 g of phosphorus pentoxide (P_2O_5) was cautiously added and the mixture was again refluxed for 10 hr to allow for formation of the vanadyl phosphate complex. The resulting solution was evaporated to about 400 ml followed by addition of 250 g of silica gel of known (−8 + 10) mesh size. Uniform deposition of the catalyst complex on the carrier was performed by heating the contents on a water bath combined with constant stirring. The free-flowing coated catalyst was then dried in an oven at 130°C and calcined in a furnace at 500°C for 4 hr.

The surface area of the catalyst as determined by the BET method was 85

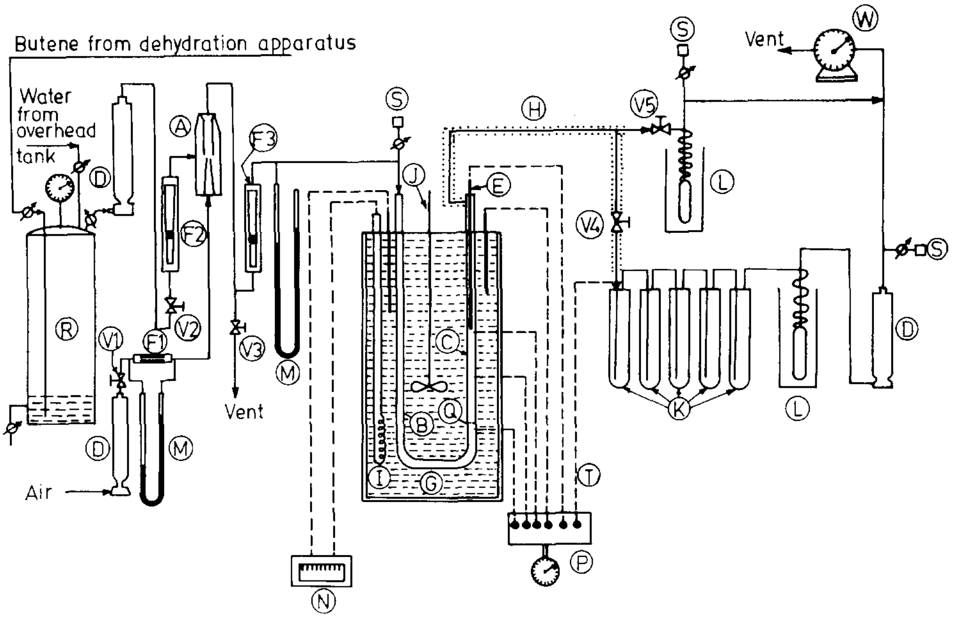

FIG. 1. Schematic diagram of experimental setup. A, Mixing chamber; B, preheater; C, reactor; D, drying tubes; E, moving thermocouple probe; F1 ... F3, flowmeters; G, salt bath; H, heating cord; I, immersion heater; J, stirrer; K, bubbler; L, cold trap; M, manometer; N, temperature controller indicator; P, temperature indicator (multipoint); Q, sieve plate; R, butene storage drum (capacity 80 liters); S, gas sampling ports; T, thermocouple; V1 ... V5, needle valves; W, wet test meter.

m^2/g. This catalyst was chosen for detailed investigation for reasons discussed elsewhere (3).

Apparatus and Procedure

The experimental assembly is schematically shown in Fig. 1. The butene gas was prepared in the laboratory and contained 53.8% *trans*-2-butene, 41.1% cis-2-butene, and the rest, 1-butene. Air and butene were passed through drying agents before use. These were metered by flowmeters, F1 and F2, respectively, and introduced into a mixing chamber. The gaseous mixture was split into two streams. One, metered by a rotameter F3, was passed through the reaction system, while the other, regulated by a valve V3, was purged to atmosphere.

The gaseous mixture to the reaction system was passed through a preheater reactor assembly, immersed in a molten salt bath whose temperature was controlled by a temperature controller within ±1°C.

The reactor, which contained a fixed bed of catalyst, was a 316 stainless-steel tube of 2.5-cm i.d. and 35-cm length. Protected chromel–alumel thermocouples were provided for the measurement of temperature at various locations as shown in Fig. 1. A moveable thermocouple was mounted along the axis of the reactor. Thus, the temperature of the catalyst bed could be measured at several locations throughout the reactor. Special precaution was taken to ensure efficient heat removal and to avoid undesirable hot spots within the reactor. Dilution of the catalyst with an inert material along with heat removal at the wall gave practically isothermal conditions. This was confirmed by measurement of temperature of the catalyst bed at various locations. The variation in temperature along the length of the reactor was no more than 2°C. Nitrogen in the feed also helped maintain isothermal conditions by acting as a diluent. It also minimized volume changes.

Exit gases from the reactor could pass through either of the two recovery paths by suitable valve adjustment. The flow-through valve V5 was allowed during the pre-steady-state period. This path was provided with a cold trap to condense maleic anhydride, followed by a gas-sampling port. The flow during the steady-state run was allowed through valve V4. The exit gases then passed through a series of two hot- and three cold-water bubblers. The 0.25-in. stainless-steel tube, joining the reactor of the bubbler, was heated by an electrical heating cord to prevent condensation of maleic anhydride. A part of off-gas from the bubblers, after passing through the cold trap and drier, was collected for analysis through a sampling port and the rest metered and vented.

Analysis

Butene isomers and butadiene were analyzed by gas chromatography using a column packed with 20% liquid paraffin on alumina. Aliquots of water scrubber solution were analyzed for acids and aldehydes. The acids were determined by titration with dilute alkali solution using phenolphthalein as an indicator and the carbonyls, by the usual oxime method. Maleic acid was estimated by precipitation as barium maleate monohydrate (*17*). The remaining acid from titration with alkali was calculated as acetic acid. Carbon dioxide, oxygen, and carbon monoxide were estimated by usual orsat analysis.

RESULTS AND DISCUSSION

Experimental Studies

Major products from the oxidation reaction were found to be butadiene, maleic acid anhydride, and carbon oxides. The Carbonyls and acetic acid amounted to less than 4% of total conversion. Inertness of the reactor was checked by conducting a few experiments in the absence of the catalyst. No oxidation product was found under these conditions. The accuracy of the data was checked by making nitrogen, oxygen, and hydrocarbon balances.

Preliminary experiments were carried out to check the reproducibility of experimental results and to estimate the range of variables best suited for kinetic analysis. The detailed results are described elsewhere (*18*). No significant decline in activity and selectivity of the catalyst was found up to about 200 hr of use. However, the adverse operating conditions of high temperature ($>400°C$) coupled with high concentration of butene in the feed (>1.0 mole%) were found to deactivate the catalyst even during a run lasting a few hours. To be safe, only those runs which were taken on relatively fresh catalyst at subcritical conditions were included in kinetic analysis. Experiments conducted at high butene conversions to study the effect of operating conditions indicated (*18*) that butene concentration in the feed and reactor temperature were the operating variables which should be controlled within rather narrow limits to obtain a substantial yield of maleic anhydride. On the other hand, space velocity could be varied within relatively wider range.

Preliminary experiments indicated the existence of physical effects unless eliminated by proper choice of operating conditions. Consequently all the kinetic experiments were performed at flow rates above 4.0×10^{-3} g-mole/sec over a catalyst of $-8 + 10$ mesh size. The influence of transport processes on reaction rate was assessed by employing a criterion derived by Mears (*19*) for the combined intraparticle and interphase case using perturbation concepts. The criterion was satisfied and hence the overall effect of diffusional

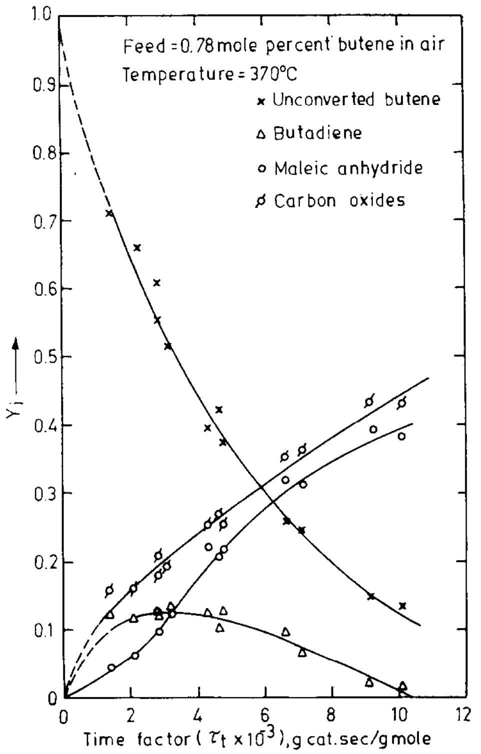

FIG. 2. Typical product distribution as a function of time factor.

resistances was unimportant under the reaction conditions. Detailed calculations are given elsewhere (*3*).

Series of kinetic experiments were carried out at varying values of space time, reaction temperature, and hydrocarbon partial pressure. The ranges of operating variables were as follows: partial pressure of butene in feed, 0.0078 to 0.018 atm; reaction temperature, 350 to 390°C; time factor, τ_t, 1.43×10^3 to 15.1×10^3 g-cat sec/g-mole.

Time factor is defined as the ratio W/F_t, where W is the weight of the catalyst, and F_t is the total molar feed rate. The partial pressure of oxygen was kept constant (0.208 atm) in all the experiments.

A typical plot of yield versus time factor for each observed component in the product is shown in Fig. 2. The yield of species A_i was calculated as follows:

$$Y_i = \frac{\text{moles of } A_i \text{ in product}}{\text{moles of reactant } A_1 \text{ in feed} \times \delta}, \quad (1)$$

where δ is the ratio of the number of carbon atoms in the reactant to the number of carbon atoms in the product.

Figure 2 shows that as butene conversion increases rapidly with time factor, yields of maleic anhydride and carbon oxides increase. The yield of butadiene, on the other hand, follows a behavior akin to that of an intermediate product. An increase in reaction temperature favored the formation of maleic anhydride as shown in Fig. 3. The yield of maleic anhydride increased slightly by increasing the partial pressure of butene in the feed to about 0.01 atm, but decreased remarkably when butene concentration was allowed to increase further (Fig. 4).

Analysis of Reaction Network

Reaction scheme. Based on a reaction mechanism proposed by previous workers (*10, 11*), the general network for butene oxidation to maleic anhydride may be written as shown.

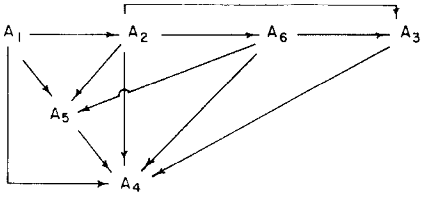

(I)

The chemical components of the above network are listed in Table 1.

For the purpose of postulating a simplified network for kinetic analysis of the reaction, the following observations from the experimental studies may be noted. (i) The yield curve for butadiene passes through a maximum. A measurable amount of butadiene is formed at low conversion of the reactant. Furan is detected only in

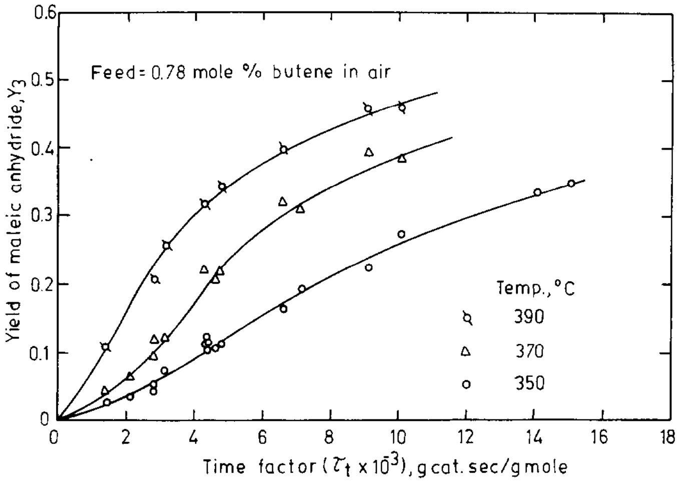

FIG. 3. Yield of maleic anhydride vs time factor with reaction temperature as a parameter.

traces (7). (ii) The organic side products are of the order of 4% of the reaction.

On the basis of observation (i), butadiene may be considered to be a primary intermediate product. Thus, the following reactions may be deleted to obtain the simplified scheme:

$$A_2 \rightarrow A_6, \quad A_6 \rightarrow A_3, \quad A_6 \rightarrow A_5, \quad A_6 \rightarrow A_4.$$

Based on observation (ii), it is permissible to combine the side products A_5 with oxides of carbon; thus making it possible to delete the following reactions:

$$A_1 \rightarrow A_5, \quad A_2 \rightarrow A_5, \quad A_5 \rightarrow A_4.$$

Further, it may be noted that the yield curve for maleic anhydride at low residence times does not reveal whether the reaction $A_3 \rightarrow A_4$ resulting in depletion of maleic anhydride is negligible or is masked by the formation reaction $A_2 \rightarrow A_3$. Experiments conducted at high residence times, when butene conversion was essentially complete (*18*), showed no significant decrease

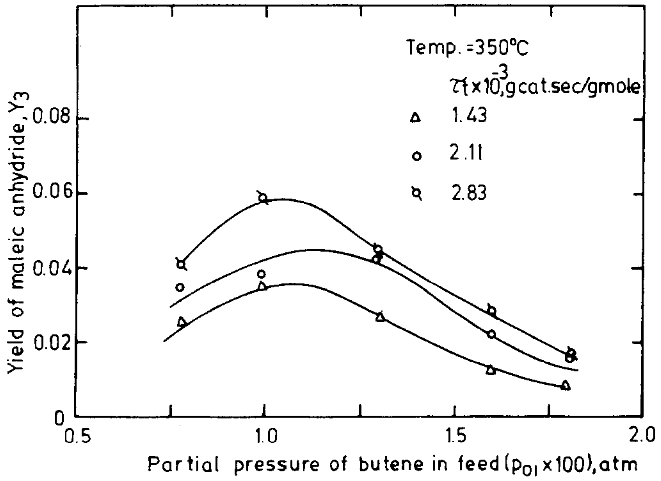

FIG. 4. Effect of butene–air ratio on the yield of maleic anhydride.

TABLE 1

List of Chemical Species

Substance	Formula	Symbol
Butene	C_2H_5-$CH=CH_2$ $CH_3CH=CHCH_3$	A_1
Butadiene	$CH_2=CHCH=CH_2$	A_2
Maleic anhydride	$\langle(\cdot CHCO)_2\rangle O$	A_3
Carbon oxides	CO, CO_2	A_4
Minor side products		
Acetic acid	CH_3COOH	
Acetaldehyde	CH_3CHO	
Acrolein	$CH_2=CHCHO$	A_5
Butyraldehyde	$CH_3CH_2CH_2CHO$	
Furan	C_4H_4O	A_6

in maleic anhydride yield, particularly at moderate temperatures. At high temperatures (>400°C), however, a slight decline in yield was noticed. This may be attributed either to destruction of maleic anhydride or to catalyst deactivation.

Based on the above discussion, the following network seems feasible.

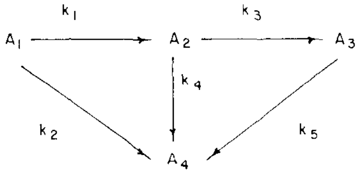

(II)

Rate of butene depletion—kinetic model. The knowledge of an adequate model is necessary for proper interpretation of kinetic data. Hougen-Watson models (*20*) have been widely used in describing solid-catalyzed reactions. Due to the lack of knowledge of the true mechanism, use of a purely empirical model (power equation) has also received wide acceptance. Recently, however, models based on theories propounded by Mars and van Krevelen (*21*) have been widely employed to interpret vapor-phase oxidation reactions. Mars and van Krevelen postulated a two-step model (redox mechanism) for hydrocarbon oxidation. The rate expression according to this model is

$$R_h = \frac{k_h k_o p_h p_o}{k_o p_o + \alpha_o k_h p_h}. \tag{2}$$

Numerous evidences in support of this theory have appeared in the literature (*4*, *22*, *23*). Recently Nakamura *et al.* (*6*) have suggested that the redox cycle between V^{5+} and V^{4+} ions is mainly concerned with the reactions from 1-butene to maleic anhydride. The steady-state adsorption model proposed by Downie *et al.* (*24*) leads to the same expression as Eq. (2).

The linearized form of Eq. (2) is

$$\frac{1}{R_h} = \frac{1}{k_h p_h} + \frac{\alpha_o}{k_o p_o}. \tag{3}$$

It would be of interest to verify if butene oxidation follows this mechanism. For this purpose, experiments were conducted varying the partial pressure of butene in feed, keeping the oxygen partial pressure constant. The rate of disappearance of butene was calculated using

$$R_h = -\frac{dY_1}{d(W/F_{01})}. \tag{4}$$

In accordance with Eq. (3), a plot of $1/R_h$ vs $1/p_h$ gives a straight line as shown in Fig. 5. More experimental evidences in support of the redox mechanism for this reaction have been discussed elsewhere (*18*).

Although the redox model is found valid over a wide range of butene concentrations studied, a butene concentration in the feed above the critical limit was found to give markedly low yields of maleic anhydride. This effect has already been discussed earlier. In addition, high butene concentration in the feed poses an explosive hazard. Due to these considerations, the concentration of butene should not usually exceed about 1.0 mole%. This condition was maintained in most of the runs taken in this investigation. Fortunately, this

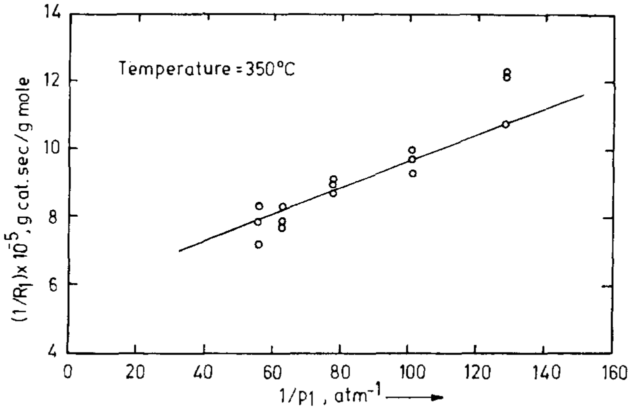

FIG. 5. Reciprocal rate of oxidation of butene as a function of reciprocal butene partial pressure.

region of practical interest allows a major simplification in the rate expression to be made. At low butene concentration, oxygen concentration being in excess, would not play any role. This is shown in Fig. 6, where log Y is plotted against time τ_t at reaction temperature 350°C. It is seen that butene disappearance follows first-order kinetics remarkably well. Similar plots were obtained for other temperatures. The conclusion, that the rate of butene oxidation follows pseudo-first-order kinetics, is in corroboration with the findings of previous workers (*7*, *10*).

Evaluation of rate constants. Owing to the presence of a large excess of oxygen in the reaction mixture, pseudo-first-order kinetics may be assumed in formulating the rate expression. Thus, for the reaction scheme II, rate equations for the four components are:

$$R_1 = -\frac{dY_1}{d\tau_1} = (k_1 + k_2)p_1, \quad (5)$$

$$R_2 = \frac{dY_2}{d\tau_1} = k_1p_1 - (k_3 + k_4)p_2, \quad (6)$$

$$R_3 = \frac{dY_3}{d\tau_1} = k_3p_2 - k_5p_3, \quad (7)$$

$$R_4 = \frac{dY_4}{d\tau_1} = k_2p_1 + k_4p_2 + k_5p_3. \quad (8)$$

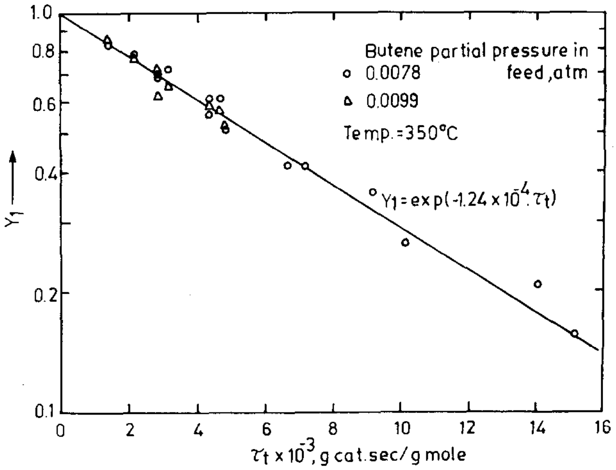

FIG. 6. First-order plot for butene depletion at 350°C.

Using the relations

$$p_i = Y_i p_{o1} = Y_i N_{o1} P \tag{9}$$

and

$$\tau_t = W/F_t = (W/F_{o1})(F_{o1}/F_t) = \tau_1 N_{o1}, \tag{10}$$

Eqs. (5) to (8) can be expressed as (at atmospheric pressure);

$$\frac{dY_1}{d\tau_t} = -(k_1 + k_2)Y_1, \tag{11}$$

$$\frac{dY_2}{d\tau_t} = k_1 Y_1 - (k_3 + k_4)Y_2, \tag{12}$$

$$\frac{dY_3}{d\tau_t} = k_3 Y_2 - k_5 Y_3, \tag{13}$$

$$\frac{dY_4}{d\tau_t} = k_2 Y_1 + k_4 Y_2 + k_5 Y_3. \tag{14}$$

Equations (11) to (14) may be integrated with the initial conditions, $Y_1 = 1$, $Y_2 = 0$, $Y_3 = 0$, $Y_4 = 0$ at $\tau_t = 0$, to give

$$Y_1 = e^{-k_{12}\tau_t} \tag{15}$$

$$Y_2 = \frac{k_1}{(k_{34} - k_{12})}\left[e^{-k_{12}\tau_t} - e^{-k_{34}\tau_t}\right], \tag{16}$$

$$Y_3 = k_1 k_3 \left[\frac{e^{-k_{12}\tau_t}}{(k_{12} - k_{34})(k_{12} - k_5)} + \frac{e^{-k_{34}\tau_t}}{(k_{34} - k_{12})(k_{34} - k_5)} + \frac{e^{-k_5\tau_t}}{(k_5 - k_{12})(k_5 - k_{34})}\right], \tag{17}$$

$$Y_4 = 1 - (Y_1 + Y_2 + Y_3), \tag{18}$$

where $k_{12} = k_1 + k_2$ and $k_{34} = k_3 + k_4$.

Preliminary estimation of rate constants was carried out by the following procedure.

(a) Equation (15) can be plotted as log Y_1 vs τ_t, as shown in Fig. 6. The slope of the straight line gives the value of k_{12} which represents the rate constant for the total disappearance of butene.

(b) Equation (12) can be rearranged to give

$$\frac{1}{Y_2}\frac{dY_2}{d\tau_t} = k_1 \frac{Y_1}{Y_2} - (k_3 + k_4). \tag{19}$$

Thus, a plot of $[(1/Y_2)(dY_2/d\tau_t)]$ vs (Y_1/Y_2) gives a straight line. The intercept and slope give the values of k_1 and $(k_3 + k_4)$, respectively.

(c) Equation (13) can be recast to give

$$\frac{1}{Y_3}\frac{dY_3}{d\tau_t} = k_3 \frac{Y_2}{Y_3} - k_5. \tag{20}$$

This gives the values of k_3 and k_5.

Refined values of rate constants at each temperature were obtained by nonlinear regression technique (*25, 26*). The objective function, S, defined by Eq. (21) was minimized by using Powell's minimization procedure (*27*).

$$S = \sum_{i=1}^{N} \sum_{j=1}^{M} (Y_{ij} - \hat{Y}_{ij})^2. \tag{21}$$

Estimation of rate constants at different temperatures revealed that values of k_5 were either negative or indistinguishable from zero and may best be set equal to zero. Accordingly, selective oxidation of butenes to maleic anhydride may be expressed by the following reaction scheme.

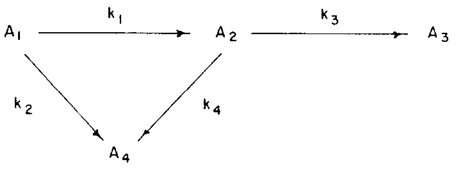

(III)

The values of the rate constants thus estimated at each reaction temperature are given in Table 2. Reasonably good fit is obtained as evidenced by small values of function S. Rate constants at different temperatures followed the Arrhenius equation. The estimated values of activation energy and the preexponential factor for each of the rate constants are given in Table 3.

The results of parameter estimation reveal that further destruction of maleic anhydride to carbon oxides is insignificant within the reaction conditions studied ($k_5 = 0$). This conclusion is in agreement with the findings of Ai *et al.* (*7, 11, 12*) which were of a qualitative nature. They found that the addition of P_2O_5 to V_2O_5 inhibits the further destruction of maleic anhydride to carbon oxides. Interestingly, studies of butadiene oxidation over MoO_3–TiO_2 catalyst by Akimoto and Echigoya (*28*) also revealed that successive oxidation of maleic anhydride does not occur, rather the anhydride and carbon dioxide are formed through different reaction paths. This explains why the yields of maleic anhydride were relatively insensitive to the time factor at higher conversions, as reported earlier (*18*).

Since an increase in temperature increases the yield of maleic anhydride which does not undergo significant destruction, the upper limit of the optimum reaction temperature would be determined essentially by the stability characteristics of the catalyst particle. Stability studies and the identification of runaway conditions, believed to be useful in determining the operating conditions giving improved yield of the desired product, are in progress.

In order to test the validity of the kinetic model, the predicted Y_i vs τ_t curves were compared with the experimental data. This is shown in Fig. 7 at 350°C. The agreement was found satisfactory at all reaction conditions studied.

TABLE 2

Estimated Values of Rate Constants

Temperature (°C)	Rate constant (g-moles/g hr atm)				S
	k_1	k_2	k_3	k_4	
350	0.30347	0.15194	0.95329	0.48119	0.03193
370	0.50328	0.23047	1.57558	0.64797	0.01638
390	0.83213	0.33426	2.50910	1.13653	0.00532

TABLE 3

Estimated Kinetic Parameters[a]

Reaction	Activation energy, E_j (kcal/g-mole)	Preexponential factor, A_j^0 (g-moles/g-cat atm hr)
I	22.1	1.5867×10^7
II	17.2	1.8866×10^5
III	20.3	1.4432×10^7
IV	18.8	1.4670×10^6

[a] $k_j = A_j^0 \exp(-E_j/R_gT_S)$; $j = 1,2,3,4$.

A comparison with the results obtained by Sunderland (*14*) at lower temperatures may be of some interest. The reaction scheme considered by him neglected butadiene as the intermediate product. He observed and took into account the further oxidation of maleic anhydride, which is not in agreement with the findings of this work nor with those of previous investigations as discussed above. The rate expression developed by Sunderland based on the Hougen–Watson model is rather cumbersome and may not be suitable for reactor design and optimization studies particularly when the reactor model accounts for pellet effects. The kinetic model developed in this investigation is believed to be useful for this purpose. Sunderland found that the rate data were adequately represented by a rate expression according to which a reaction between adsorbed oxygen and gaseous 2-butene was controlling. It is interesting to note that this mechanism is not very different from the two-stage redox mechanism which postulates the oxidation of hydrocarbon in the gas phase by the oxygen ion of the oxide lattice.

CONCLUSIONS

The integral reactor immersed in a molten salt bath was found satisfactory for kinetic studies of this reaction. Pre-

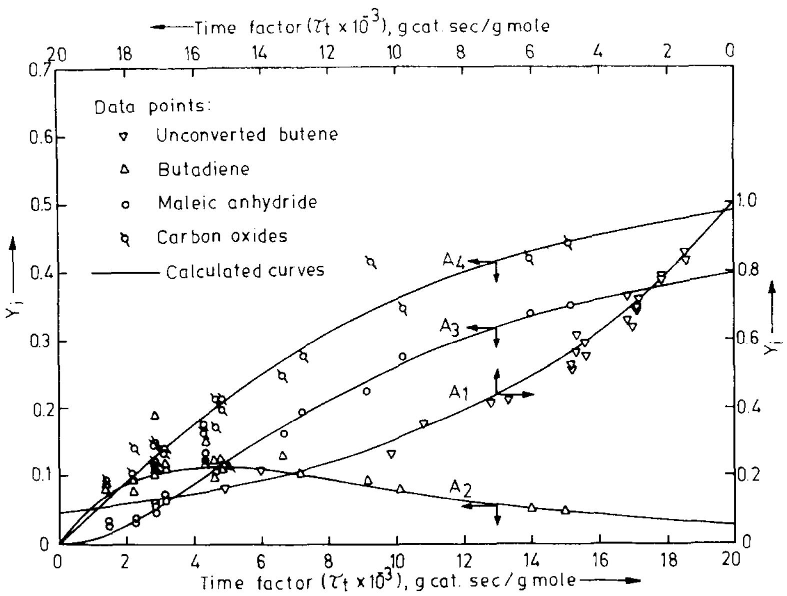

FIG. 7. Testing adequacy of rate expressions—product distribution at 350°C.

liminary diagnostic tests suggested insignificant transport effects under the chosen operating conditions. Oxidation of butene was found to follow a two-stage redox model. The mechanism of the reaction was observed to be in agreement with that proposed by previous workers. Maleic anhydride is formed by oxidation of butene via butadiene as the principal intermediate product. No significant oxidation of maleic anhydride to carbon oxides occurs under the reaction conditions studied. Pseudo-first-order rate equations could be fitted to each of the reaction steps at low concentrations of butene in the feed. The basic kinetic parameters were thus determined.

REFERENCES

1. Ushio, S., *Chem. Eng.* (*N. Y.*) **78** (21), 107 (1971).
2. Sherwin, M., *Chem. Tech.*, April, 225 (1974).
3. Varma, R. L., Ph.D. thesis, Indian Institute of Technology, Kanpur, 1976.
4. Hucknall, D. J., "Selective Oxidation of Hydrocarbons." Academic Press, New York, 1974.
5. Dente, M., Ranzi, E., Quiroza, O. D., and Biardi, G., *Chem. Ind.* (*Milan*) **55**(7), 563 (1973); *Chem. Abstr.* **80**, 47200 g.
6. Nakamura, M., Kawai, K., and Fujiwara, Y., *J. Catal.* **34**, 345 (1974).
7. Ai, M., *Bull. Chem. Soc. Japan* **43**(11), 3490 (1970).
8. Ai, M. and Suzuki, S., *Bull. Chem. Soc. Japan* **47**(12), 3074 (1974).
9. Sampson, R. J., and Shooter, *D., Oxid. Combust. Rev.* **1**, 225 (1965).
10. Ostroushko, V. I., Kernos, Yu. D., Ioffe, I. I., *Neftekhimiya* **12**(3), 362 (1972); *Chem. Abstr.* **77**, 100433b.
11. Ai, M. Harada, K., and Suzuki, S., *Kogyo Kagaku Zasshi* **73**(3), 524 (1970); *Chem. Abstr.* **73**, 44631t.
12. Ai, M., Boutry, P., and Moutarnal, R., *Bull. Soc. Chim. Fr.* **8–9**, 2775 (1970).
13. Ai, M., Boutry, P., Montarnal, R., and Thomas, G., *Bull. Soc. Chim. Fr.* **8–9**, 2783 (1970).
14. Sunderland, P., *Ind. Eng. Chem. Prod. Res. Develop.* **15**(2), 90 (1976).
15. Kerr, R. O. (Petro–Tex Chemical Corp), U.S. 3,366,648; U.S. 3,385,796 (1968).
16. Nakamura, M. Kawai, K., and Fujiwara, Y. (Kuraray Co., Ltd.), *Japan Kokai* **7**, 441, 291 (1974); *Chem. Abstr.* **83**, 59938d.
17. Milas, N. A., and Walsh, W. L., *J. Amer. Chem. Soc.* **57**, 1389 (1935).
18. Varma, R. L., and Saraf, D. N., *Ind. Chem. Engr. Trans.* **20**, 42 (1978).
19. Mears, D. E., *Ind. Eng. Chem. Process Des. Develop.* **10**, 541 (1971).
20. Hougen, O. A., and Watson, K. M., "Chemical Process Principles." Part 3. Wiley, New York, 1947.

21. Mars, P., and van Krevelen, D. W., special supplement to *Chem. Eng. Sci.* **3**, 41 (1954).
22. Balasubramanian, S., and Viswanath, D. S., *Ind. Eng. Chem. Fundam.* **14**(3), 158 (1975).
23. van der Wiele, K., and van den Berg, P. J., *J. Catal.* **39**, 437 (1975).
24. Downie, J. Shelstad, K. A., and Graydon, W. F., *Canad. J. Chem. Eng.* **39**, 201 (1961).
25. Himmelblau, D. M., "Process Analysis by Statistical Methods." Chap. 6. Wiley, New York, 1970.
26. Ball, W. E., and Groenweghe, L. C. D., *Ind. Eng. Chem. Fundam.* **5**, 181 (1966).
27. Powell, M. J. D., *Comput. J.* **7**, 303 (1965).
28. Akimoto, M., and Echigoya, E., *Bull. Japan Petrol. Inst.* **16**(1), 8 (1974).